The Relationship Between MRI Parameters and Spinal Compressive Loading

Jie Zhou[1], Fadi Fathallah[1(✉)], and Jeffery Walton[2]

[1] Department of Biological and Agricultural Engineering, University of California Davis, Davis, CA 95616, USA
fathallah@ucdavis.edu

[2] NMR Facility, University of California Davis, Davis, CA 95616, USA

Abstract. Intervertebral disc (IVD) is a leading source of Low back pain (LBP). The health and functions of the IVD are determined by the inherent biomechanical properties of the IVD and its interaction with external mechanical loading. Quantitative Magnetic Resonance Imaging (MRI) parameters have the potential in detecting loading-induced changes in biomechanical properties of the IVD. $T_{1\rho}$, T_2 and Apparent Diffusion Coefficient (ADC) were obtained with a 7T MRI scanner from 20 functional spinal units (FSU) before and after receiving compressive loading of 263.27 N for 60 min. Compressive loading was found to significantly reduce $T_{1\rho}$ and T_2 but not ADC, indicating that $T_{1\rho}$ and T_2 had the potential to detect loading-induced changes in biomechanical properties of the IVD. These parameters may provide more sensitivity and specificity to understand the injury mechanism of the IVD and contribute to early diagnosis of IVD degeneration.

Keywords: MRI parameters · Spinal compressive loading · Intervertebral disc

1 Introduction

Low back pain (LBP) remains a major socioeconomic problem, and one of the leading sources is the IVD [1]. Injuries to the disc itself can cause discogenic pain [2]. Also, compromise in IVD biomechanics may impair neuromuscular control of postural stability and make other spinal tissues more vulnerable to injury, and thus may cause LBP [3–5].

The biomechanical properties of the IVD are largely determined by the concentration of the proteoglycan (PG) in the nucleus pulposus (NP) of the IVD [6]. When subjected to compressive loading, water is expelled out from the NP, which increases the concentration of PG and the associated osmotic pressure, such that the compressive load can be balanced and an equilibrium can be restored. When the load is removed, water re-imbibes into the NP, which reduces osmotic pressure corresponding to the magnitude of the load, hence, achieving a new equilibrium state [7] (Fig. 1).

The health and functions of the IVD are determined by both the inherent tissue properties (e.g. PG content, osmotic pressure and hydration) and their interaction with external mechanical loading. The inherent properties of the IVD are not directly determinable in-vivo; whereas, quantitative MRI parameters, such as spin–lattice

S. Bagnara et al. (Eds.): IEA 2018, AISC 820, pp. 579–585, 2019.
https://doi.org/10.1007/978-3-319-96083-8_76

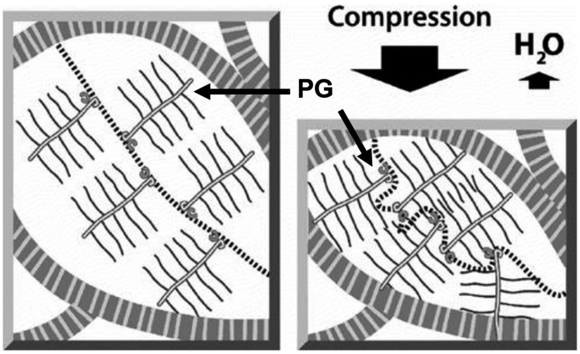

Fig. 1. The expulsion of water from the IVD

relaxation in the rotating frame ($T_{1\rho}$), spin–spin relaxation (T_2) and Apparent Diffusion Coefficient (ADC) may extract pertinent information about biomechanical properties of the IVD, which is useful for understanding the effects of loading on the health and functions of the IVD [7]. Therefore, the objective of the current study is to investigate how compressive loading changes $T_{1\rho}$, T_2 and ADC in the NP of the IVD.

2 Methods

2.1 Specimens

Porcine cervical spines were harvested from young pigs freshly-slaughtered and used as the specimens, due to the similarity in morphometry, geometry, and curvature to the human lumbar spine [8]. The cervical spines were then wrapped in phosphate buffered saline (PBS) soaked gauze, sealed in plastic bags, and frozen at −20 °C until testing. They were thawed for approximately 12 h before testing and each cervical spine was dissected to obtain 2 functional spinal units (FSU) (C3-C4 and C5-C6) [9]. Each FSU consists of 2 adjacent vertebral bodies, the IVD and all connecting ligamentous tissues between them. The posterior ligaments were removed to isolate loading to the IVD (Fig. 2). A total of 20 FSUs were harvested from 10 pigs, the average (standard deviation) of the weight and age were 10.92 kg (1.49 kg) and 45.4 days (3.58 days), respectively.

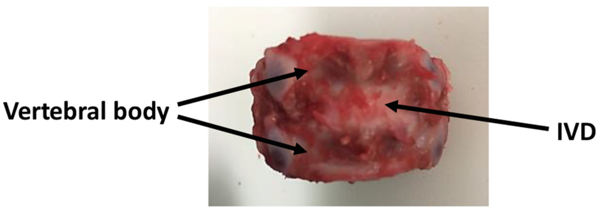

Fig. 2. The structure of Functional Spinal Unit (FSU)

2.2 Experimental Design

A repeated-measures experimental design was performed. $T_{1\rho}$, T_2 and ADC were obtained before and after receiving compressive load of 263.27 N for 60 min. This load magnitude corresponds to 1500 N on human lumbar IVD according to the scaling factor in IVD areas between the porcine cervical and human lumbar discs [10]. The 3D-SSPP software (University of Michigan, Ann Arbor, Michigan, USA) was used to determine such 1500 N compressive load when simulating a 50th percentile male worker holding a 23 kg load. The 23 kg has been suggested as the maximum recommended weight limit by NIOSH lifting equation [11].

2.3 Experimental Procedure

A computer controlled load-displacement device was built to apply compressive loading inside the MRI scanner (Fig. 3). FSUs were casted and drilled, then secured into the sample holder with pins. PBS soaked gauze was used to wrap the FSU to maintain the hydration of the IVD (Fig. 4a), sample holder was assembled into the tube (Fig. 4b), and the whole apparatus was installed onto the opening of the MRI bore with an aluminum flange plate (Fig. 4c). And the electrical components (e.g. pressure sensors and DAQ), pneumatic system (e.g. pneumatic actuator, proportional pneumatic control valve and compressed air supply) and LabView software were set up to achieve force-displacement control and monitor (Fig. 4d).

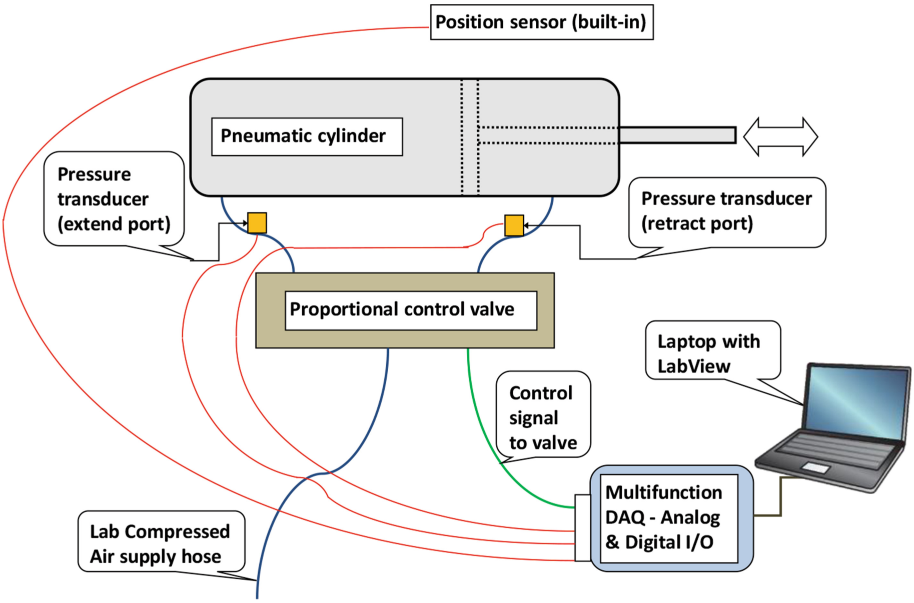

Fig. 3. The diagram of the apparatus

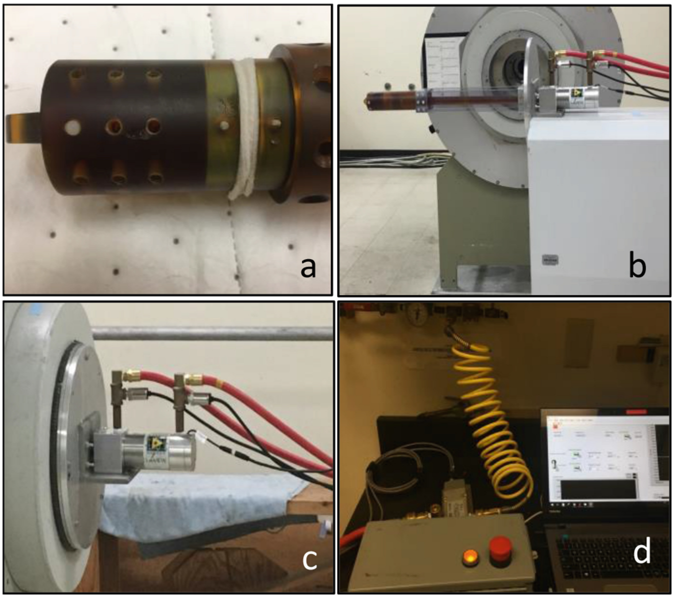

Fig. 4. The computer controlled pneumatic load-displacement apparatus

The 7T Bruker Biospec imaging instrument (Bruker Inc., Billerica, MA, USA) in the NMR facility of UC Davis was used for imaging. During MRI imaging, a series of T_2-weighted images were first performed with 5 different spin echo times (TE ranged from 15 to 75 ms, with 15 ms increments), while repetition time (TR) was kept constant at 2000 ms. A series of diffusion-weighted images (DWI) with b values range from 200 to 1000 s/mm^2 (with 200 s/mm^2 increments) were then performed, TE and TR were kept constant at 24 ms and 1000 ms, respectively. At last, five $T_{1\rho}$-weighted images were performed with spin lock time (TSL) ranging from 15 to 75 ms (15 ms increments), TE and TR were kept constant at 20 ms and 1000 ms, respectively (Fig. 5). The spin lock frequency (FSL) was kept at 500 Hz. All images were obtained from the sagittal plane of the specimen, the slice thickness was set at 1 mm for T_2 and $T_{1\rho}$ imaging, and 2.26 mm for DWI. The IVD was kept compressed during imaging to maintain a constant loading condition.

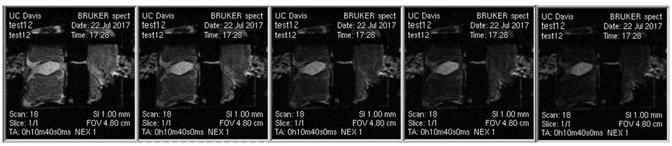

Fig. 5. The individual $T_{1\rho}$ images with each of the five TSL

The Bruker built-in ParaVision software was used to analyze the acquired images to obtain the MRI parameters. At first, the region of interest (ROI) was defined to cover only the NP of the IVD, and the signal intensity in the ROI of the series of images was calculated. The signal intensity of these images was then fitted with the exponential decay equation of each MRI parameter, thus the MRI parameters (i.e. $T_{1\rho}$, T_2 and ADC) can be calculated.

2.4 Statistical Analysis

Paired-t tests were performed to compare $T_{1\rho}$, T_2 and ADC obtained before and after the compressive loading. The α value of 0.05 was set as the significance criteria. Minitab software (Minitab Inc., State College, Pennsylvania, USA) was used to conduct all the statistical analyses.

3 Results

The effects of compressive loading on MRI parameters were demonstrated in Table 1. Significantly reduced $T_{1\rho}$ (from 112.43 to 93.47 ms) was observed in the NP of the IVD after receiving the compressive loading. T_2 was also significantly decreased from 50.78 ms in the baseline condition to 33.51 ms in the compressed condition. However, ADC was not significant affected (P = 0.353).

Table 1. Measured MRI parameters (and standard errors) with and without loading. Bold fonts indicate significant differences.

	$T_{1\rho}$ (ms)	**T_2 (ms)**	ADC (mm^2/s)
Baseline	**112.43 (6.22)**	**50.78 (4.70)**	0.002887 (0.000054)
Compressed	**93.47 (5.12)**	**33.51 (3.45)**	0.002790 (0.000084)

4 Discussion

The $T_{1\rho}$ relaxation time of the NP can be estimated as the weighted $T_{1\rho}$ relaxation times of all the chemical components that made up of the NP [12]. NP primarily constitutes of water (80%) and PG (15%) [13], change in either composition can affect the $T_{1\rho}$ relaxation time. In the current study, the applied compressive load is believed to expel water content out from the NP, which can be detected by $T_{1\rho}$ relaxation time. Also, the decrease in $T_{1\rho}$ relaxation time indicated reduced water content in NP, which is in line with the finding from previous studies [14, 15].

It is not surprising that T_2 relaxation time decreases with greater IVD degeneration grades [16], since the grading system was created according to the IVD morphology with T_2-weighted images [17]. Loss of water content is one of the most immediate and apparent changes, which occur at early stage of IVD degeneration [18]. Therefore, in the current study, T_2 relaxation time is also significantly reduced by the applied compressive loading, since such loading can expel water out from the NP of the IVD and induce early degenerative changes [7].

ADC was found to be affected by the IVD composition and matrix integrity [19]. In the current study, although water content was reduced in the NP of the IVD, ADC was not significantly affected by the applied compressive load, presumably due to the expelled water was not sufficient enough to alter ADC.

In summary, $T_{1\rho}$ and T_2 relaxation times were found sensitive to the applied compressive load, which indicates their potential to detect the biomechanical changes in the NP of the IVD induced by the external mechanical loading. Therefore, they may provide more sensitivity and specificity to understand the injury mechanism of the IVD and contribute to early diagnosis of IVD degeneration, thus help reduce the prevalence of LBP.

Acknowledgement. This project was partially funded by the Western Center for Agricultural Health and Safety (WCAHS) with NIOSH Grant No. 2U54OH007550.

References

1. Fourney DR, Andersson G, Arnold PM, Dettori J, Cahana A, Fehlings MG, Chapman JR (2011) Chronic low back pain: a heterogeneous condition with challenges for an evidence-based approach. Spine 36:S1–S9
2. Brisby H (2006) Pathology and possible mechanisms of nervous system response to disc degeneration. J Bone Joint Surg 88(suppl 2):68–71
3. Panjabi MM (2006) A hypothesis of chronic back pain: ligament subfailure injuries lead to muscle control dysfunction. Eur Spine J 15(5):668–676
4. Zhou J, Ning X, Fathallah F (2016) Differences in lumbopelvic rhythm between trunk flexion and extension. Clin Biomech 32:274–279
5. Ning X, Zhou J, Dai B, Jaridi M (2014) The assessment of material handling strategies in dealing with sudden loading: the effects of load handling position on trunk biomechanics. Appl Ergon 45(6):1399–1405
6. Adams MA, Roughley PJ (2006) What is intervertebral disc degeneration, and what causes it. Spine 31(18):2151–2161
7. Urban JP, Winlove CP (2007) Pathophysiology of the intervertebral disc and the challenges for MRI. J Magn Reson Imaging 25(2):419–432
8. Noguchi M, Gooyers CE, Karakolis T, Noguchi K, Callaghan JP (2016) Is intervertebral disc pressure linked to herniation?: an in-vitro study using a porcine model. J Biomech 49(9):1824–1830
9. Nikkhoo M, Kuo Y, Hsu Y, Khalaf K, Haghpanahi M, Parnianpour M, Wang J (2015) Time-dependent response of intact intervertebral disc–In Vitro and In-Silico study on the effect of loading mode and rate. Eng Solid Mech 3(1):51–58
10. Beckstein JC, Sen S, Schaer TP, Vresilovic EJ, Elliott DM (2008) Comparison of animal discs used in disc research to human lumbar disc: axial compression mechanics and glycosaminoglycan content. Spine 33(6):E166–E173
11. Waters TR, Putz-Anderson V, Garg A, Fine LJ (1993) Revised NIOSH equation for the design and evaluation of manual lifting tasks. Ergonomics 36(7):749–776
12. Levine, H., & Slade, L. (Eds.). (2013). Water Relationships in Foods: Advances in the 1980 s and Trends for the 1990 s (Vol. 302). Springer Science & Business Media

13. Raj PP (2008) Intervertebral disc: anatomy-physiology-pathophysiology-treatment. Pain Pract 8(1):18–44
14. Johannessen W, Auerbach JD, Wheaton AJ, Kurji A, Borthakur A, Reddy R, Elliott DM (2006) Assessment of human disc degeneration and proteoglycan content using T1ρ-weighted magnetic resonance imaging. Spine 31(11):1253
15. Souza RB, Kumar D, Calixto N, Singh J, Schooler J, Subburaj K, Majumdar S (2014) Response of knee cartilage T1rho and T2 relaxation times to in vivo mechanical loading in individuals with and without knee osteoarthritis. Osteoarthritis Cartilage 22(10):1367–1376
16. Takashima H, Takebayashi T, Yoshimoto M, Terashima Y, Tsuda H, Ida K, Yamashita T (2012) Correlation between T2 relaxation time and intervertebral disk degeneration. Skeletal Radiol 41(2):163–167
17. Griffith JF, Wang YXJ, Antonio GE, Choi KC, Yu A, Ahuja AT, Leung PC (2007) Modified Pfirrmann grading system for lumbar intervertebral disc degeneration. Spine 32(24): E708–E712
18. Stokes IA, Iatridis JC (2004) Mechanical conditions that accelerate intervertebral disc degeneration: overload versus immobilization. Spine 29(23):2724–2732
19. Antoniou J, Demers CN, Beaudoin G, Goswami T, Mwale F, Aebi M, Alini M (2004) Apparent diffusion coefficient of intervertebral discs related to matrix composition and integrity. Magn Reson Imaging 22(7):963–972